PERGAMON

Available at
www.ElsevierComputerScience.com
POWERED BY SCIENCE DIRECT

Pattern Recognition 37 (2004) 351–361

PATTERN RECOGNITION
THE JOURNAL OF THE PATTERN RECOGNITION SOCIETY
www.elsevier.com/locate/patcog

Extraction of karyocytes and their components from microscopic bone marrow images based on regional color features

Xi-Wen Zhang[a,*], Ji-Qiang Song[b], Michael R. Lyu[b], Shi-Jie Cai[a]

[a] *State Key Laboratory of Novel Software Technology, Department of Computer Science and Technology, Nanjing University, Nanjing, 210093, People's Republic of China*
[b] *Department of Computer Science and Engineering, The Chinese University of Hong Kong, Shatin, N.T., Hong Kong SAR, People's Republic of China*

Received 18 September 2002; accepted 16 July 2003

Abstract

Extracting karyocytes and their components from microscopic bone marrow images is prerequisite for computer-aided early diagnosis of hemopathy. Most existing methods assume all pixels belonging to a karyon region or a cytoplasm region have similar colors. Practically, the color of neither a karyon nor a cytoplasm in a microscopic image is homogeneous in the pixel level. Therefore, the regional color features of a region are emphasized in this paper. Based on this observation, we propose a novel method to karyocyte extraction that first identifies a karyon by 4-connected block growing from a karyon feature block, then identifies feature blocks of its cytoplasm based on the extracted karyon, and finally extracts all cytoplasm regions by growing the cytoplasm feature blocks. Combining the karyon region and the corresponding cytoplasm regions can attain a complete karyocyte. Experimental results show that the proposed method is effective and robust.

Keywords: Image segmentation; Karyocyte extraction; Microscopic bone marrow image; Regional color features; Feature-block growing

1. Introduction

Hemopathy is a frequent yet dangerous disease that endangers human health. The identification and enumeration of karyocytes in stained bone marrow smears can provide very important information for early diagnosing and treating these diseases [1]. In order to identify a hemopathy type that determines the choice of drugs and therapy schemes, each karyocyte in smears should be classified according to its cell series, growing stage, pathological properties and normal properties [2]. Bone marrow smears contain all kinds of leukocytes and erythrocytes, the analysis of which needs to consider a lot of karyocyte features to classify karyocytes. Manually locating, classifying and enumerating karyocytes in bone marrow smears is tedious and time-consuming. Moreover, due to the limitation of human energy, manual process can only examine a small fraction of the smear, and cannot ensure keeping high accuracy constantly. Computer-aided automatic analysis of microscopic bone marrow images is a promising way to overcome the weakness of manual operations.

Generally, automatic microscopic image analysis to aid the diagnosis of hemopathy consists of four steps: (1) extract each karyocyte and its components from the microscopic image. (2) Extract normal and abnormal features from the extracted karyocytes. (3) Classify the karyocytes according to their normal features and abnormal ones. (4) Diagnose the case according to the classification results. Among these four

* Corresponding author. Laboratory of Human–Computer Interaction, Institute of Software, The Chinese Academy of Sciences, Building 4 Room 305, Beijing 100080, China. Tel.: +86-010-62540434; fax: +86-010-62652533.
E-mail address: zxw19@sina.com (X.-W. Zhang).

0031-3203/$30.00
doi:10.1016/j.patcog.2003.07.007

steps, the first step is prerequisite to the succeeding analyses. However, it is difficult due to the complexity of karyocyte color features (texture), the variation of karyocyte shape and the interference of non-interesting objects. Therefore, the automatic extraction of karyocytes and their components is not performed ideally so far [1]. This paper is to address this problem.

Most existing methods are based on the assumption that all pixels belonging to a karyon region or a cytoplasm region have similar colors, so they use pixel-level operators, e.g., thresholding approaches [3], edge-based approaches [4–6], region-based approaches [7–10], model-based approaches [4–6,11,12]. Unfortunately, in a microscopic bone marrow image, the color of neither a karyon region nor a cytoplasm region is homogeneous in the pixel level. Therefore, these methods are not enough to extract karyocytes effectively and accurately in such images. However, humans can easily identify karyons or cytoplasms since each karyon region or each cytoplasm region is of a homogeneous texture regarding the color and its distribution in a region. Based on this observation, the regional color features are emphasized in this paper. If a karyon region or a cytoplasm region is divided into equal-sized blocks and each block is represented by its color distribution, the differences among these blocks are much smaller. The colors and the color distributions of blocks within the same karyon region or the same cytoplasm region are similar. This observation will help to extract karyon regions and cytoplasm regions fast and accurately. Consequently, this paper proposes a novel approach to extract karyocytes and their components based on the regional color features.

The rest of this paper is organized as follows. Section 2 reviews the previous work related to karyocyte extraction. Section 3 describes the definition of a feature block of an interesting region and the block-growing algorithm. Section 4 applies the approach proposed in Section 3 to the extraction of karyons, cytoplasms and their karyocytes. In Section 5, detailed experimental results and performance analyses are reported, and some comparisons with other approaches are also given. Section 6 draws our conclusions.

2. Related work and our analyses

Existing karyocyte extraction approaches can be roughly classified into four classes according to their underlying techniques.

(1) *Thresholding-based approaches*: Heijden [3] proposed an image segmentation approach for complete leukocytes based upon multiple gray-level thresholding. Unfortunately, its performance falls down in the presence of erythrocytes that may often have similar gray-level values to the cytoplasm of leukocytes.

Although the thresholding method is computationally cheap and fast, the threshold is only derived from the statistical distributions of local or global pixel properties, and the spatial information is neglected. Thus, a post-processing is needed to label connected regions, fill small holes in regions, and remove small regions. It is possible to perform those tasks using morphological operations. However, it is often difficult to choose appropriate structuring elements that will achieve satisfactory results [13].

(2) *Region-based approaches*: Region-based approaches [14] is to group pixels of the same or similar brightness or color into regions according to given criteria of homogeneity. The neighboring pixels of a given pixel (or region) are merged into the given region if they satisfy the homogeneity criteria. Region-based approaches include region splitting and merging approaches [7,8], seeded region growing approaches [9,10].

In order to incorporate a priori knowledge during region extraction, Adams and Bischof [9] introduced a seeded region growing algorithm. A priori knowledge is represented by the placement of a seed in the interesting region. These seeds then grow by absorbing single pixels based on a similarity criterion. For the correct seed placement, they proposed the option of semi-interactive operation where seeds are manually placed. Due to the pixel-by-pixel growing [7–10], the results are sensitive to noise.

(3) *Edge-based approaches*: Cong and Parvin [4] extracted karyon regions based on partial boundary information. The approach uses local feature activities in the form of step-edge segments, roof-edge segments, and concave corners to construct a set of initial hypotheses. They converted the segmentation problem into a constrained optimization problem. Yang and Jiang [5] proposed a segmentation approach to extract karyocytes from images under noisy conditions by combining kernel-based dynamic clustering and a genetic algorithm. It is based on cell boundaries. Garrido and Blanca [6] proposed a cell image segmentation method based on edges under severe noisy conditions.

An edge detector usually produces borders almost, but not completely, closed. The subsequent edge linking is to close the borders of regions based upon an edge detected image. This is a very difficult task as it is often not clear which edges are of interest and which are not [13].

(4) *Model-based approaches*: The edge-based approaches [4,5] model each karyocyte boundary as an elliptic shape to extract karyocyte regions after detecting edges. Garrido and Blanca [6] proposed a deformable template approach for cell image segmentation based on edges. Aus et al. [11] proposed a karyocyte segmentation algorithm driven by the model of karyocyte structure, which assumes that a karyocyte consists of one karyon surrounded by an area of cytoplasm, and that any area of a karyon cannot be shared by two or more karyocytes. Park and Keller [12] proposed an approach combining the watershed approach and the snake model to extract the boundaries of karyocytes. But this approach does not further extract karyon regions and cytoplasm regions.

Previous related work on karyocyte extraction has not provided complete information of karyocytes. They either

extract karyons without extracting cytoplasms, or extract karyocytes without extracting their components. In fact, karyocyte classification cannot be performed correctly without complete information of karyocytes. Current methods need much post-processing to extract complete karyons or cytoplasms. We think that a priori knowledge in color textures of karyons and cytoplasms should be incorporated into the extraction process. Obviously, this can improve the entirety of extraction results and furthermore greatly reduce post-processing. Our new approach is designed in the following principles.

(a) Karyon regions and cytoplasm regions are extracted in their entirety.
(b) The extracted regions are complete (with fewer holes), accurate (with acceptable boundary location errors), and correct (without mis-connecting karyons and cytoplasms of different karyocytes).
(c) The colors of karyons (or cytoplasms) in different images, even in the same image, are different. The extraction method should be able to adapt to this color variance.
(d) The criteria of homogeneity should be non-sensitive to the color difference of pixels in an interesting region.
(e) A priori knowledge of karyons and cytoplasms should be incorporated effectively to improve reliability of the extraction and reduce the burden of post-processing.

3. Feature block and its growing

In a microscopic bone marrow image, neither the color of a karyon region nor that of a cytoplasm region is homogeneous in the pixel level, as shown in Fig. 1. Fig. 1b is the maximum karyon region cropped from the original image shown in Fig. 1a. Its 3D surface in the green channel is illustrated in Fig. 1c. The karyon region in the green channel is more homogeneous than the other two channels. But, the surface is not even and uniform, thus its corresponding region is not homogeneous in the pixel level. Current methods of karyon or karyocyte extraction based on pixel-level operations are prone to oversegmenting karyons or karyocytes due to the inhomogeneity in pixel colors.

However, humans recognize a karyon region or a cytoplasm region mainly depending on its regional color homogeneity, that is to say, the regional color features, including the principal color in the region and its density and distribution, impress human vision most. Following this observation, we propose to use a feature block to identify the regional color features and extract the interesting region based on the feature block growing.

3.1. Definition of a feature block

A feature block is a square sub-image of the original bone marrow image, which identifies the global color features of an interesting region such as a karyon region or a cytoplasm region. To define the feature block of an interesting region, three color-related definitions for a block are given first.

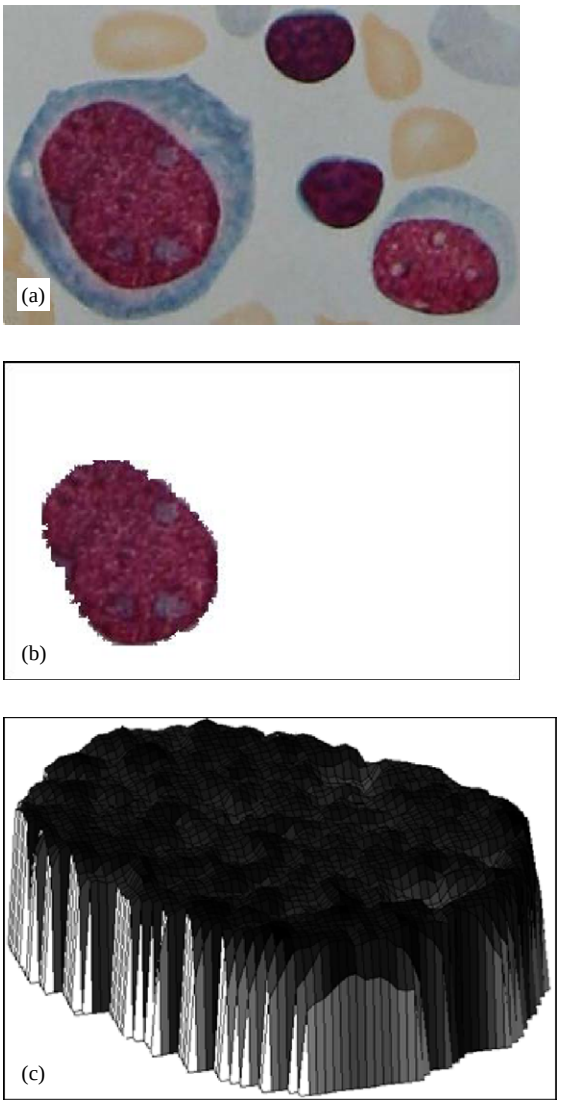

Fig. 1. Original microscopic bone marrow image. (a) Orginal image. (b) The maximum karyon region cropped from the original image. (c) 3D surface of the maximum karyon region image in the green channel.

(1) *Principal color* (PC): PC is the color with the most pixels in the block, which can represent the color of this block.
(2) *Density of principal color* (PCD): PCD is the ratio of the number of pixels with PC over that of all pixels in the block, which reflects the saturation of the principal color in a block.

(3) Homogeneity of principal color (PCH): After dividing a block into nine equal-sized square sub-blocks, PCH is the ratio of the minimal PCD of nine sub-blocks over the PCD of the block, which reflects the extent of homogeneous distribution of PC.

Definition 1. A feature block of an interesting region is a square sub-image that can represent the global color features of the region. It must satisfy the following three constraints simultaneously:

(1) PC is within a predefined color range, i.e., $\text{min\_PC} \leqslant \text{PC} \leqslant \text{max\_PC}$.
(2) PCD is larger than a predefined threshold, i.e., $\text{PCD} \geqslant \text{min\_PCD}$.
(3) PCH is larger than a predefined threshold, i.e., $\text{PCH} \geqslant \text{min\_PCH}$.

The thresholds min_PC, max_PC, min_PCD and min_PCH, are predefined according to interesting regions. To determine these predefined thresholds, we first manually collect a large number of interesting regions that are sub-images cropped from original images. Then PC, PCD and PCH of each sub-image are automatically calculated using the above definitions. Finally, min_PC and max_PC are set to be the minimum and the maximum of all PCs, respectively. Min_PCD is set to be the minimum of all PCDs, and min_PCH is set to be the minimum of all PCHs. Therefore, for each type of interesting region, there is a set of predefined thresholds. We provide two sets of thresholds for karyon regions and cytoplasm regions in microscopic bone marrow images, respectively, in Section 4.

According to the positional relationship between a block and an interesting region, a block can be classified into three categories according to the following three definitions: the internal block, the boundary block, and the external block.

Definition 2. An internal block is entirely inside the interesting region, which means all its sub-blocks are inside the interesting region as well. A feature block must be an internal block.

Definition 3. A boundary block is partially inside the interesting region. There are at least one and at most eight sub-blocks locating entirely inside the interesting region.

Definition 4. An external block is entirely outside the interesting region, which means all its sub-blocks are outside the interesting region.

Since the principal colors of different karyocytes vary, after identifying a feature block of an interesting region, the classification thresholds of three categories of blocks are calculated based on the parameters of the feature block. Considering the impact from noisy pixels, the conditions of these blocks are not so strict as that of the feature block. The thresholds are relaxed as $\text{min\_PC}' = \text{PC} - \varepsilon_C$, $\text{max\_PC}' = \text{PC} + \varepsilon_C$, $\text{min\_PCD}' = \text{PCD} - \varepsilon_D$, $\text{min\_PCH}' = \text{PCH} - \varepsilon_H$, where ε_C, ε_D and ε_H are small offsets from PC, PCD and PCH of the feature block, respectively. Thus, a block (or sub-block) is inside the interesting region on conditions that: (1) PC ranges between $\text{min\_PC}'$ and $\text{max\_PC}'$, (2) $\text{PCD} \geqslant \text{min\_PCD}'$, and (3) $\text{PCH} \geqslant \text{min\_PCH}'$.

3.2. Feature block growing

To extract an interesting region, we first detect a feature block of the interesting region from the image. Then, the feature block grows by merging successive connected internal blocks and boundary blocks until no more satisfactory blocks can be found. After the growing terminates, the feature block, the internal blocks and all the internal sub-blocks of the boundary blocks recorded during the growing form the interesting region. The detailed algorithm of the feature-block growing is described by the following C++ pseudo-code:

```
//Initialization
ActiveBlock = the feature block;
Label the pixels within the ActiveBlock as processed.
GrowingList = Empty;
BOOL Stop = False;
//Block growing
WHILE (NOT Stop) {
  Check which directions (leftward/rightward/
    upward/downward) of the ActiveBlock
    can be grown;
  FOR (each direction that can be grown) {
    ThisBlock = the connected block of the
      ActiveBlock in current direction;
    IF (ThisBlock is not external AND the
      pixels within ThisBlock are unprocessed) {
      Add ThisBlock to the tail of the
        GrowingList;
      Set the pixels within
        ThisBlock as processed;
    }
  }
  IF (GrowingList is empty)
    Stop = True;
  ELSE {
    ActiveBlock = the first block of
      the GrowingList;
    Remove the first block from
      the GrowingList;
  }
}
```

In the above algorithm, one direction of the active block can be grown on condition that there is at least one internal sub-block on the corresponding side of the active block.

4. Extraction of karyocytes and their components

In our application, we do not consider the karyocytes with more than one karyons. Theoretically, there are two available orders for extracting karyon regions and cytoplasm regions, i.e., karyon regions first or cytoplasm regions first. A karyocyte contains only one karyon. However, there may be more than one cytoplasm regions belonging to one karyocyte since the karyon often offsets from the center of the karyocyte and its shape is irregular. If a cytoplasm region is first extracted, we have to detect its own karyon and then find other cytoplasm regions belonging to this karyon to form the complete karyocyte. This is, however, not a straightforward and efficient way. Since cytoplasm regions always surround their own karyon region, it is reasonable to first extract a karyon region and then to extract the surrounding cytoplasm regions based upon the extracted karyon region.

4.1. Karyon extraction

According to the medical statistic result about karyocytes in bone marrows [2], the minimum of karyon diameters exceeds 5 μm, and the maximum exceeds 20 μm. If the magnification of microscope to acquire the bone marrow images is 1000× and the image capturing resolution is 5 pixels per μm, a karyon region in an image contains at least 400 pixels, whereas a nucleolus region or a perforation region contains at most 80 pixels. Thus, the widths of blocks cannot be larger than 20 pixels. We set the heuristic rules of the karyon extraction based on these facts.

Block size is critical to the overall performance since it directly affects the accuracy of the resulting regions, the processing time and the boundary approximation precision. According to the analysis of the relationship between the block size and the karyon extraction performance (provided in Section 5), we set the width of a block to be 9 pixels, which can achieve the best performance result.

Furthermore, the thresholds for feature block growing are determined. Considering the complete chromatic information of an interesting region, we use three color channels of the chromatic image for karyon extraction. The thresholds min_PC, max_PC, min_PCD and min_PCH in red, green and blue channels are calculated, respectively, after analyzing many karyon regions. The thresholds for karyon extraction are set as follows: for the red channel, $\min\_PC = 44$, $\max\_PC = 165$, $\min\_PCD = 0.30$, $\min\_PCH = 0.85$, $\varepsilon_C = 10$, $\varepsilon_D = 0.10$, $\varepsilon_H = 0.05$; for the green channel, $\min\_PC = 13$, $\max\_PC = 99$, $\min\_PCD = 0.30$, $\min\_PCH = 0.85$, $\varepsilon_C = 10$, $\varepsilon_D = 0.10$, $\varepsilon_H = 0.05$; and for the blue channel, $\min\_PC = 29$, $\max\_PC = 120$, $\min\_PCD = 0.30$, $\min\_PCH = 0.85$, $\varepsilon_C = 10$, $\varepsilon_D = 0.10$, $\varepsilon_H = 0.05$.

We first identify a feature block of a karyon region by coarse-to-fine detection in the original image. The image is scanned coarsely using a block row-by-row stepping 6 pixels. If attaining a candidate block that satisfies three conditions of the feature block for karyons, we perform a fine scan around the candidate block stepping 3 pixels to detect the best feature block, which is the one with the maximum sum of PCDs in three color channels and the maximum sum of PCHs in three color channels. After identifying the karyon feature block, its PC, PCD, and PCH in each color channel can be attained. Thus, we can set the thresholds in each color channel for extracting the karyon region: $\min\_PC' = PC - \varepsilon_C$, $\max\_PC' = PC + \varepsilon_C$, $\min\_PCD' = PCD - \varepsilon_D$, $\min\_PCH' = PCH - \varepsilon_H$, which makes the thresholds adaptive to the current karyon. Then, we extract the karyon region by growing the feature block using the algorithm stated in Section 3.2. A group of connected internal blocks and boundary blocks is attained after the growing terminates. Therefore, the karyon region is finally extracted as a group of connected homogeneous blocks.

4.2. Cytoplasm extraction

The cytoplasm extraction is also performed in the three color channels of the chromatic image. Same as the karyon extraction, we set the width of a block to be 9 pixels. After analyzing many cytoplasm regions as stated in Section 3.1, the thresholds for extracting cytoplasm regions are set as follows: for the red channel, $\min\_PC = 58$, $\max\_PC = 152$, $\min\_PCD = 0.30$, $\min\_PCH = 0.85$, $\varepsilon_C = 15$, $\varepsilon_D = 0.10$, $\varepsilon_H = 0.15$; for the green channel, $\min\_PC = 83$, $\max\_PC = 172$, $\min\_PCD = 0.30$, $\min\_PCH = 0.85$, $\varepsilon_C = 15$, $\varepsilon_D = 0.10$, $\varepsilon_H = 0.15$; and for the blue channel, $\min\_PC = 99$, $\max\_PC = 158$, $\min\_PCD = 0.30$, $\min\_PCH = 0.85$, $\varepsilon_C = 15$, $\varepsilon_D = 0.10$, $\varepsilon_H = 0.15$.

Although one karyocyte perhaps contains more than one cytoplasm regions, they all surround the karyon of the karyocyte. So, we do not need to visit every pixels of the image to detect the cytoplasm regions. Instead, we start from the outmost blocks of the detected karyon region. It is possible that there are more than one cytoplasm feature blocks for a karyon.

The cytoplasm feature blocks are identified as the connected unprocessed blocks of the outmost block of the karyon region, which are with the regional color features that are predefined for the extraction of cytoplasm feature blocks. Then, a set of thresholds in each color channel for extracting a cytoplasm region are calculated based on a cytoplasm feature block, which is adaptive to the current cytoplasm region. The cytoplasm regions are extracted by growing from the cytoplasm feature blocks with the algorithm stated in Section 3.2. Therefore, the cytoplasm, which may contain more than one region, is finally extracted as at least one group of connected homogeneous blocks.

4.3. Karyocyte extraction

After extracting a karyon region and its corresponding cytoplasm region (or regions), the boundary of the karyocyte is either one of cytoplasm if the karyon is totally surrounded by the cytoplasm, or the combination of one of the

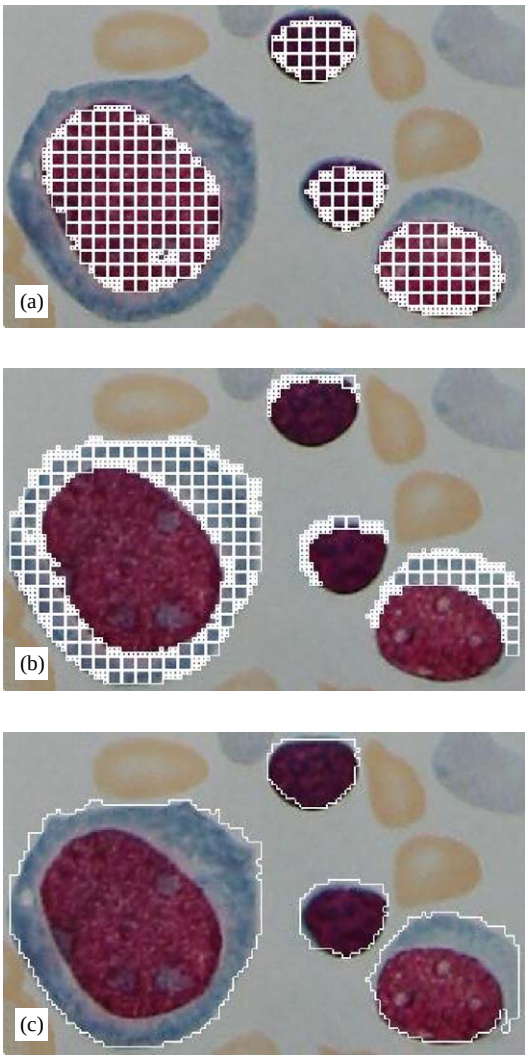

Fig. 2. Karyocytes and their components extracted using the proposed approach. (a) Internal blocks and sub-blocks of the karyon regions overlapping the image. (b) Internal blocks and sub-blocks of the cytoplasm regions overlapping the image. (c) Boundaries of the karyocyte regions overlapping the image.

cytoplasm and one of the karyon. Thus, we can attain a complete karyocyte by combining the karyon and the cytoplasm.

After attaining a karyocyte, we go on to scan the image for the next karyocyte by the above karyon extraction and cytoplasm extraction processes until no karyon feature block is detected from the image. The karyon regions, cytoplasm regions, and karyocyte regions detected from the image of Fig. 1 are shown in Fig. 2. Fig. 2a and Fig. 2b show the detected karyon regions and cytoplasm regions, respectively, where the bigger squares are the internal blocks, and smaller ones are the internal sub-blocks of the boundary blocks. Although the two smaller karyon regions and the two larger ones have obvious different colors, they are all detected since the extraction thresholds are adaptive to each region. Fig. 2c shows the boundary of the extracted karyocyte regions overlapping the original image.

5. Performance analyses

Based on the approach introduced above, a software prototype has been developed in Visual C++ R6.0 by authors. This section presents performance evaluation in terms of experimental results with real images and quantitative analyses using the third party protocols.

5.1. Experimental results

Many microscopic bone marrow images have been tested on this software prototype. More experimental results are shown in Fig. 3. The colors and shapes of karyon regions are various, so are those of cytoplasm regions. The extracted karyon regions are shown in Fig. 3a, where the boundary are precise and the nucleoli and perforations are handled well. Fig. 3b is the result of extracted cytoplasm regions, which demonstrates that the proposed approach can handle various positional relationships between karyons and their cytoplasms. With the correct extraction results of both the karyon regions and the cytoplasm regions, the karyocyte regions are also extracted correctly and easily, as shown in Fig. 3c.

To make a quantitative evaluation on the extracted results, we must obtain the ground-truth data at first. As the ground-truth data cannot be obtained by some automatic processing, we manually detected the karyon regions (Fig. 4a), cytoplasm regions (Fig. 4b) and karyocyte regions (Fig. 4c) aided by a professional hematologist. The region boundaries are displayed using white pixels overlapping on the original image.

We employ two well-known image segmentation evaluation protocols that ranked high in Zhang's survey [15]: Relative Ultimate Measurement Accuracy for Area ($\mathrm{RUMA_A}$) [16] and Probability of Error (PE) [17], to evaluate our extraction results. $\mathrm{RUMA_A}$ is defined as

$$\mathrm{RUMA_A} = \frac{|R_A - S_A|}{R_A} \times 100\%,$$

where R_A is the area of the ground-truth object and S_A is the area of the extracted object. Thus, $\mathrm{RUMA_A}$ indicates the relative percents of the area discrepancy. The smaller the $\mathrm{RUMA_A}$ is, the higher the extraction accuracy is. PE is defined as

$$\mathrm{PE} = P(O) \times P(B|O) + P(B) \times P(O|B),$$

where $P(B|O)$ is the probability of error in classifying objects as background, $P(O|B)$ is the probability of error in classifying background as objects, and $P(O)$ and $P(B)$ are a priori probabilities of objects and background in

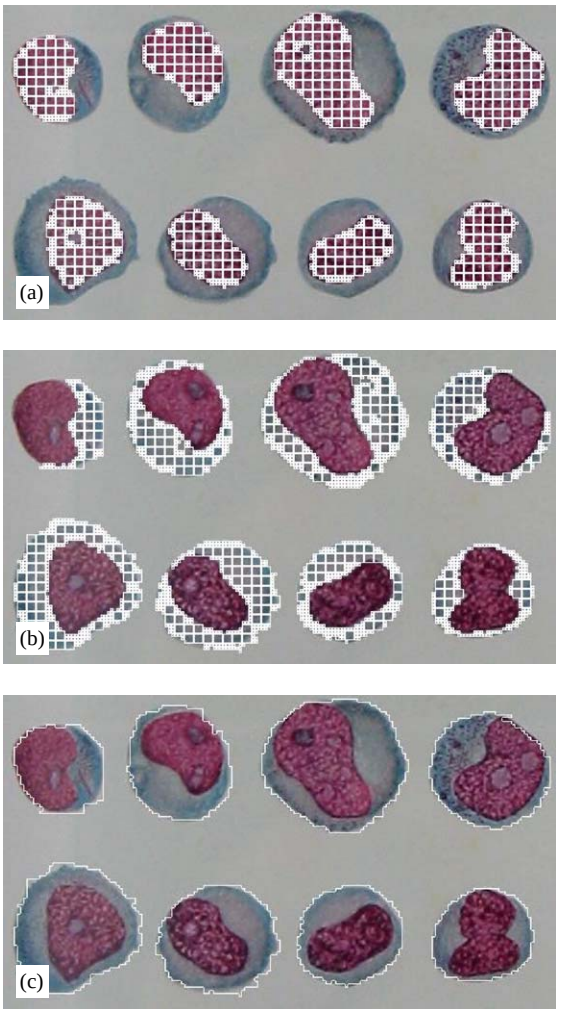

Fig. 3. Experimental results on the microscopic bone marrow image. (a) Internal blocks and sub-blocks of the karyon regions overlapping the image. (b) Internal blocks and sub-blocks of the cyoplasm regions overlapping the image. (c) Boundaries of the karyocyte regions overlapping the original image.

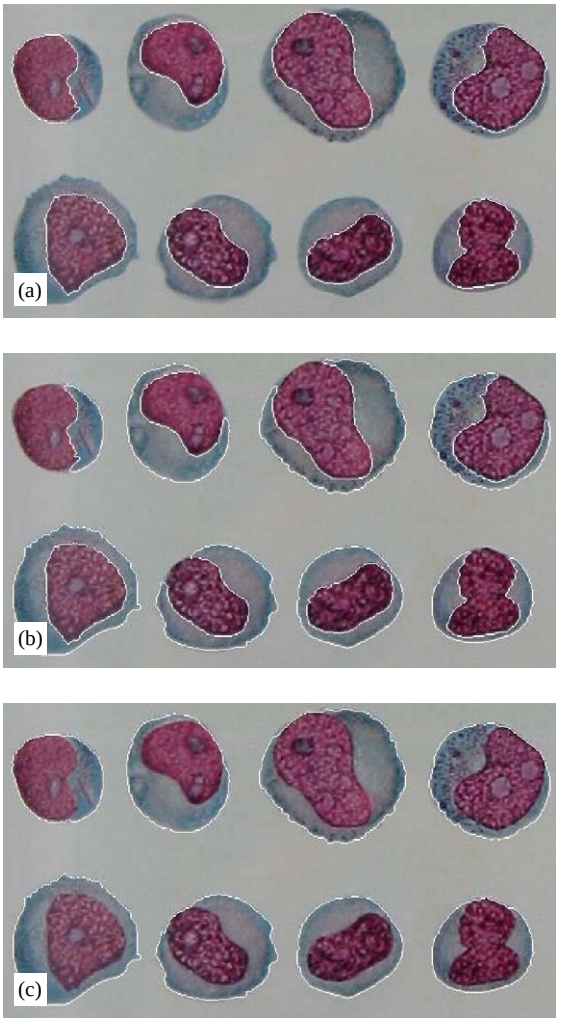

Fig. 4. Manually detected ground-truth results. (a) Ground-truth boundaries of the karyon regions. (b) Ground-truth boundaries of the cytoplasm regions. (c) Ground-truth boundaries of the karyocyte regions.

images. Also, the smaller the PE is, the higher the extraction accuracy is.

The evaluation results of the pixel discrepancy of extracted karyocyte regions, karyon regions, and cytoplasm regions (Fig. 3) comparing with the ground-truth data (Fig. 4) are given in Table 1. The order of labeling the karyocytes is row-by-row and top down.

Table 1 demonstrates that the extraction accuracy (i.e., 1−extraction discrepancy) of the proposed approach is high. Actually, the average extraction discrepancies in PE and in $RUMA_A$ on 100 testing images are below 5% and below 10%, respectively.

The processing time is another important performance index. Table 2 lists the processing time (tested on a PC with PIII 800 MHz CPU and 256M RAM) of extracting karyon regions and cytoplasm regions, respectively, in several images. We find that the processing time is proportional to the number and area of karyocytes, but not the size of image. This is because we use the coarse-to-fine scanning scheme to detect the feature blocks, which passes the non-interesting regions quickly. The processing time for cytoplasm regions is less than that for karyon regions since detecting the feature blocks of cytoplasm regions does not need to scan the image.

5.2. Block size selection

Block size is the major parameter in the proposed approach. It impacts the performance in three aspects: the pixel

Table 1
Evaluation of extraction discrepancy of our approach

Item Label	Karyocyte region		Karyon region		Cytoplasm region	
	$RUMA_A$(%)	PE (%)	$RUMA_A$(%)	PE (%)	$RUMA_A$(%)	PE (%)
1	1.0	2.7	8.7	0.5	12.3	3.7
2	0.3	2.9	6.4	0.6	3.4	4.7
3	1.3	3.3	6.9	0.7	4.2	5.8
4	0.9	1.7	8.7	0.5	1.9	3.3
5	3.5	5.8	14.4	0.3	11.8	9.8
6	4.6	5.1	14.7	0.2	11.1	7.5
7	1.0	2.9	11.1	0.3	3.2	4.6
8	0.7	1.9	8.2	0.4	2.1	3.4

Table 2
Processing time for experimental images

Item Image	Image size (pixel^2)	Number of karyocytes	Time for karyons (s)	Time for cytoplasms (s)	Total time for karyocytes (s)	Time per karyocyte (s)
1 (Fig. 1)	335 × 207	4	2.35	1.26	3.61	0.90
2 (Fig. 3)	517 × 294	8	4.79	3.16	7.95	0.99
3	698 × 686	21	13.95	4.21	18.61	0.87
4	912 × 681	26	19.47	6.33	25.80	0.99
5	930 × 625	23	16.93	5.25	22.18	0.96
6	930 × 649	28	19.05	6.67	25.72	0.92

discrepancy or accuracy of resultant regions, the processing time, and the approximate boundary scale. Generally, a smaller block (as long as it is) will increase accuracy of detected regions but take much more processing time and be more sensitive to noisy pixels. Since the boundaries of detected regions are approximated by the sides of blocks and sub-blocks, smaller blocks are sure to produce more precise boundaries. To determine which block size is the best, we design a Block Size Priority (BSP) computation as follows:

$$\mathrm{BSP} = 1 - (\alpha \times \mathrm{Discrepancy} + \beta \times \mathrm{Time} + \gamma \times \mathrm{BoundaryScale}),$$

where α, β and γ are the performance weights of the region discrepancy, the processing time, and the boundary approximation scale, respectively. The higher the BSP is, the higher the extraction accuracy is. Since the aim of our application is to identify the karyocytes and to analyze their components and shapes, the region accuracy is important. The processing time is also important to meet the requirement of real-time application. However, the boundary approximation scale is less important because small approximation errors do not affect the shape analysis. Therefore, we set $\alpha = 0.4$, $\beta = 0.4$, and $\gamma = 0.2$ in our block size selection. When calculating BSP, each performance value is divided by the maximum of its column to be normalized into [0,1].

Table 3
Performance profiles over different block sizes

Block size (pixels)	$RUMA_A$(%)	Processing time (s)	Boundary scale (pixels)	BSP
6	9.2	10	2	0.316
9	9.3	5	3	0.332
12	10.7	3	4	0.244
15	11.4	2	5	0.160

Table 3 shows the performance profiles for Fig. 3 when the block size varies from 6 to 15, where block size must be a multiple of 3. The boundary approximation scale is the width of a sub-block. The result is the BSP of 9 pixels is the highest; therefore, we set the block size to be 9 pixels in our approach.

5.3. Comparisons

Fig. 5 shows segmentation results using three other methods. Fig. 5a shows the segmentation result from the grayscale image of Fig. 1a using Ostu's thresholding approach [18]. In order to extract the karyon regions correctly,

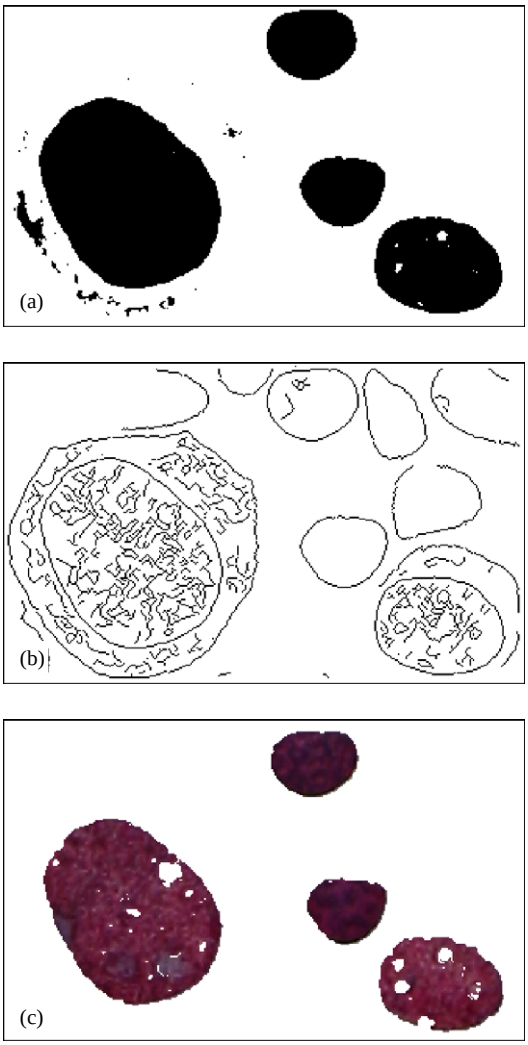

Fig. 5. Segmentation results using three other methods. (a) Thresholding result with Ostu's approach. (b) Extracting edges with Canny's detector. (c) Regions extracted from the original image using the improved seeded region growing algorithm.

there is still a post-processing to delete black noisy regions and to fill holes. For example, Park and Keller [12] combine the watershed approach and the snake model to extract the boundaries of karyocytes based on thresholding images. Heavy computation is needed to extract accurate boundaries by searching many candidate points. Moreover, it is difficult to further extract the cytoplasm regions. Fig. 5b shows the edges extracted from the grayscale image using Canny's edge detector [19]. Obviously, it is hard to extract the boundaries of the karyocyte, those of karyon regions, and those of cytoplasm regions from such noisy edges. Based on extracted edges, the approaches proposed in [4,5] utilize an elliptic model to guide region extraction, and the approach proposed in Ref. [6] uses a deformable template to do so. These approaches also need large search. Fig. 5c shows the karyon regions extracted from the original image using the seeded region growing algorithm [9,10]. Due to the pixel-level operation, the two bigger karyon regions contain some holes and have less accurate boundaries. Comparing with the boundaries shown in Fig. 2, we find that our proposed approach produces more satisfactory results.

The proposed approach and four other approaches are further compared in nine aspects, including processing level, utilization of a priori knowledge, result type, post-processing burden, noise sensitivity, computational cost, region accuracy, shape adaptability, and texture adaptability. The other approaches are the thresholding-based approach [18], the edge-extraction-based approach [19], the model-based approach [12], and the seeded region growing approach [9,10]. The comparison results among these approaches and our proposed approach are listed in Table 4, which shows that our proposed approach has more advantages than other approaches, especially, in region accuracy, shape adaptability and texture adaptability. Therefore, the proposed approach can achieve satisfactory results for extracting arbitrary-shaped textured karyon regions and cytoplasm regions in microscopic bone marrow images.

5.4. Discussions

With the above experimental results and performance analyses, we conclude that the proposed approach has three major advantages:

(1) Using regional color features instead of using the color of each pixel, this approach is not sensitive to the inhomogeneous colors in the pixel level and to the local noises.
(2) The feature block growing is able to get the entire interesting region; therefore, no post-processing is needed.
(3) The extraction thresholds are adaptive to each interesting region; therefore, the proposed approach can extract regions of different principal colors in the same image.

The current limitation of the proposed approach is that the extraction speed (about 1 s per karyocyte) is not fast enough to perform real-time analyses. This requires the further optimization in the algorithm implementation.

6. Conclusions

This paper introduces the regional color features, including the principal color, the principal color density, and the principal color homogeneity, to improve the adaptability to the regional color inhomogeneity in the pixel level. This paper further proposes a feature-block growing algorithm based on the regional color homogeneity constraints. With this algorithm, one can successfully detect a region in its

Table 4
Comparison among five karyocyte-extraction approaches

Approach Characteristic	Thresholding-based approach [18]	Edge-detection-based approach [19]	Model-based approach [12]	Seeded region growing approach [9,10]	The proposed approach
Processing level	Pixel	Pixel and its neighbors	Pixels	Pixel and its neighbors	Block (A group of pixels)
Utilization of a priori knowledge	No	No	Much	Little	Much
Result type	Pixel	Edge pixel	Regional boundaries	Region	Region
Post-processing burden	Connected-region labeling & screening	Edge-pixel linking & screening	No	Region splitting & merging	No
Noise sensitivity	High	High	High	Low	Very low
Computational cost	Low	Moderate	High	Moderate	Moderate
Region accuracy	Low	Low	High	Moderate	High
Shape adaptability	High	High	Low	High	High
Texture adaptability	Low	Low	Low	Low	High

entirety no matter it is of uniform color or of homogeneous principal color. In this paper, we apply the proposed approach to the extraction of karyocytes and their components in microscopic bone marrow images. Detecting karyon regions in the block level rather than in the pixel level improves the extraction accuracy and efficiency. The accurate karyon regions act as the starting points of extracting the surrounding cytoplasm regions, which further improves the extraction speed. Complete information of a karyocyte is finally attained with combining the karyon and its corresponding cytoplasm. We have tested the proposed approach using many microscopic bone marrow images on the software prototype developed by authors. The performance analyses are reported in detail, including the experimental results, the performance evaluation and the comparison with other methods. The analyses confirm that the proposed approach is effective and robust.

7. Summary

Counting of different classes of karyocytes in bone marrow smears plays an important role in the diagnosis of hemopathy. An automatic differential counter based on computer vision makes it possible to perform the medical test rapidly, accurately and economically. Although the classification of karyocytes is a classical field of pattern recognition, the success of classification mainly depends on the correct and accurate extraction of karyocyte regions. Extracting karyocytes and their components from microscopic bone marrow images is prerequisite to provide original data for subsequent classification of karyocytes. Most existing methods assume that all pixels belonging to a karyon region or a cytoplasm region have similar colors, so they use pixel-level operators, e.g., thresholding, edge detection, seeded region growing, and model-based approaches. Practically, the color of neither a karyon nor a cytoplasm in a microscopic bone marrow image is homogeneous in the pixel level. This paper presents a novel method to extract karyocyte regions based on the regional color features. The regional color features of a region are its homogeneous textures, i.e., the color and its distribution in a region. The proposed method first identifies a karyon by 4-connected block growing from a karyon feature block, then identifies feature blocks of its cytoplasm based on the extracted karyon, and finally extracts all cytoplasm regions by growing the cytoplasm feature blocks. Combining the karyon region and the corresponding cytoplasm regions can attain a complete karyocyte. Experimental results show that the proposed method is effective and robust for detecting arbitrary-shaped textured karyon regions and cytoplasm regions in microscopic bone marrow images.

Acknowledgements

The work described in this paper was substantially supported by a grant from the Research Grants Council of the Hong Kong Special Administrative Region, China (Project No.CUHK4182/03E).

References

[1] P. Sobrevilla, E. Montseny, J. Keller, White blood karyocyte detection in bone marrow images, in: Proceedings of the 18th International Conference of the North American Fuzzy Information Processing Society, New York, USA, June 10–12, 1999, pp. 403–407.
[2] E. Beutler, M.A. Lichtman, B.S. Coller, T.J. Kipps, URI Seligsohn, Williams Hematology, 6th Edition, McGraw-Hill Publishing Company, USA, New York, 2001.
[3] F. van der Heijden, Image based measurement systems, Object Recognition and Parameter Estimation, Wiley, West Sussex, England, 1995, pp. 215.
[4] G. Cong, B. Parvin, Model-based segmentation of nuclei, Pattern Recognition 33 (8) (2000) 1383–1393.

[5] F. Yang, T. Jiang, Karyocyte image segmentation with kernel-based dynamic clustering and an ellipsoidal karyocyte shape model, J. Biomed. Informatics 34 (2) (2001) 67–73.
[6] A. Garrido, N.P. de la Blanca, Applying deformable templates for cell image segmentation, Pattern Recognition 33 (5) (2000) 821–832.
[7] S.L. Horowitz, T. Pavilidis, Picture segmentation by a tree traversal algorithm, J. Assoc. Comput. Mach. 23 (2) (1976) 368–388.
[8] X. Wu, Adaptive split-and-merge segmentation based on piecewise least-square approximation, IEEE Trans. Pattern Anal. Mach. Intell. 15 (8) (1993) 808–815.
[9] R. Adams, L. Bischof, Seeded region growing, IEEE Trans. Pattern Anal. Mach. Intell. 16 (6) (1994) 641–647.
[10] A. Mehnert, P. Jackway, An improved seeded region growing algorithm, Pattern Recognition Lett. 18 (10) (1997) 1065–1071.
[11] H.M. Aus, H. Harms, V. ter Meulen, U. Gunzer, Statistical evaluation of computer extracted blood karyocyte features for screening populations to detect leukemias, in: P.A. Devjver, J. Kittler (Eds.), Pattern Recognition Theory and Applications, Springer, Berlin, Heidelberg, 1987.
[12] J. Park, J.M. Keller, Snakes on the watershed, IEEE Trans. Pattern Anal. Mach. Intell. 23 (10) (2001) 1201–1205.
[13] Pascal Christopher Bamford, Segmentation of cell images with application to cervical cancer screening, a dissertation, University of Queensland, 1999, pp. 52–53.
[14] H.D. Cheng, X.H. Jiang, Y. Sun, J. Wang, Color image segmentation: advances and prospects, Pattern Recognition 34 (12) (2001) 2259–2281.
[15] Y.J. Zhang, A survey on evaluation methods for image segmentation, Pattern Recognition 29 (8) (1996) 1335–1346.
[16] Y.J. Zhang, Evaluation and comparison of different segmentation algorithms, Pattern Recognition Lett. 18 (10) (1997) 963–974.
[17] S.U. Lee, S.Y. Chung, R.H. Park, A comparative performance study of several global thresholding techniques for segmentation, Comput. Vision Graphics Image Process. 52 (2) (1990) 171–190.
[18] N. Ostu, A threshold selection method from gray-level histogram, IEEE Trans. Syst. Man Cybern. 9 (1) (1979) 62–66.
[19] J. Canny, A computational approach to edge detection, IEEE Trans. Pattern Anal. Mach. Intell. 8 (6) (1986) 679–698.

About the Author—XI-WEN ZHANG was born in Liaoning, P.R. China, in 1971. He received the Bachelor degree in Chemical Equipment and Mechanics from Fushun Institute of Petrol in 1995 July and the Ph.D. degree in Mechanical Manufacturing and Automation from Dalian University of Technology in 2000 October. From 2000 October to 2002 September, he worked as a post doctor in Computer Science and Technology at State Key Lab. of Novel Software Technology, Department of Computer Science and Technology, Nanjing University. Since 2002 October he has been with Institute of Software, the Chinese Academy of Sciences, and has become an associate research professor since 2003 January. He is a member of IEEE and IEEE_CS. His research interests include medical image analysis, computer vision, artificial intelligence, human computer interaction and understanding of scanned engineering drawings.

About the Author—JI-QIANG SONG was born in Jiangsu, P.R. China, in 1974. He received the B.S. degree in Computer Science and the Ph.D. degree in Computer Science and Application from Nanjing University in 1996 and 2001, respectively. Currently, he is a Postdoctoral Fellow at Department of Computer Science and Engineering, the Chinese University of Hong Kong. His research interests include graphics recognition, automatic interpretation of engineering drawings, image processing and video processing. He has published over 20 papers in these areas. He is a member of IEEE, IEEE Computer Society and IAPR.

About the Author—MICHAEL R. LYU received the B.S. (1981) in electrical engineering from National Taiwan University, the M.S. (1985) in computer engineering from University of California, Santa Barbara, and the Ph.D. (1988) in computer science from University of California, Los Angeles. He is a Professor at the Computer Science and Engineering Department of the Chinese University of Hong Kong. He worked at the Jet Propulsion Laboratory, Bellcore (now Telcordia) and Bell Labs, and taught at the University of Iowa. His research interests include software reliability engineering, distributed systems, image processing and video processing, fault-tolerant computing, web technologies, web-based multimedia systems, and wireless communications. He has published over 130 papers in these areas. He is the editor for two book volumes: Software Fault Tolerance, published by Wiley in 1995 and the Handbook of Software Reliability Engineering, published by IEEE and McGraw-Hill in 1996. He has been an associated editor of IEEE Transactions on Reliability, IEEE Transactions on Knowledge and Data Engineering, and Journal of Information Science and Engineering.

About the Author—SHI-JIE CAI is a Professor at the Department of Computer Science & Technology, Nanjing University. He graduated from Department of Mathematics from Nanjing University in 1967. His research interests include computer graphics, graphics recognition, image processing, and document analysis and recognition.